Centre de Recherches Mathématiques
CRM Proceedings and Lecture Notes

Coherent Control: Principles and Semiclassical Implementations

Victor S. Batista and Paul Brumer

ABSTRACT. Optimal control of quantum systems seeks to optimize dynamics to reach a desired target. The underlying physics of such quantum control involves aspects of interference between indistinguishable quantum pathways to the same final state. The physics of such interference based control, termed coherent control, is here reviewed and applied to control of proton transfer in a large molecular system. Emphasis is placed on both the physics of coherent control and on the semiclassical computational techniques required to predict coherent control in large systems.

1. Introduction

The vast majority of lectures at this workshop are dedicated to optimal control of quantum systems. Such work has as its main goal the optimization of target yields, with only secondary concern for the underlying physical mechanisms that make the control efficient. By contrast, work over the past sixteen years in *coherent control*[**1, 2**] has focused on the underlying quantum mechanisms that allow for control in molecular systems. Specifically, it has focused on the role and utility of quantum interference between indistinguishable pathways to the target state, in controlling quantum systems. Its advantage lies in the emphasis on the physics associated with quantum control, which allows for the development of a number of general control principles.

Coherent control has been successfully applied to a wide variety of processes, including molecular photodissociation, atomic ionization, bimolecular collision processes, control of chirality in chemistry, nanoscale deposition of molecules on surfaces, control of chaotic dynamics, controlled quantum chaotic diffusion, controlled dynamics in an optical lattice, the construction of decoherence free subspaces, with applications using both continuous wave as well as pulsed lasers. These topics, as well as others, are thoroughly discussed in two recent monographs[**1, 2**]. In addition, we have recently analyzed optimal control from the coherent control perspective[**3**].

1991 *Mathematics Subject Classification.* Primary 37N35, 81Q99; Secondary 81V55.
Key words and phrases. Coherent Control, Quantum Control, Semiclassical Mechanics.
This work was supported by the U.S. Office of Naval Research.

Below we briefly review some of the basics of coherent control. We then describe, as an example of a forefront coherent control study, the application of coherent control to proton transfer in a large molecule, an example typical of a vast array of interesting processes that involve large molecules. Emphasis is placed upon both the nature of the dynamics required to treat large molecules, specifically semiclassical mechanics, and upon the ability to control systems in the presence of deleterious dephasing. The latter is particularly important since practical applications of quantum control will necessitate studies in the domain where decoherence is ubiquitous.

To introduce the principle of coherent control we consider the control of the dynamics of molecular photodissociation, i.e. the process:

$$A + BC \leftarrow ABC \rightarrow AB + C.$$

Here the molecule ABC, where A, B, C denote atoms or molecular components, is excited by a photon and dissociates to one of the two indicated products. Interest is in controlling the relative probabilities of producing the products.

1.1. Photodissociation. Consider a molecule interacting with a pulse of coherent light where the light is described in terms of an electric field $\mathbf{E}(z,t)$ propagating along the z axis:

$$\mathbf{E}(z,t) = \hat{\boldsymbol{\epsilon}}\varepsilon(z,t) \tag{1}$$

where

$$\varepsilon(z,t) = \int_{-\infty}^{\infty} d\omega \epsilon(\omega) \exp[-i\omega(t - z/c)] \ . \tag{2}$$

is the strength of the field and $\hat{\boldsymbol{\epsilon}}$ is the polarization direction vector. The quantity ω denotes the frequency. The dynamics of the system is described by a time dependent Hamiltonian, $H(t) = H_M + H_{MR}$. Here H_M is the (radiation free) material Hamiltonian and H_{MR} is the matter-radiation interaction, given in the dipole approximation as

$$H_{MR} = -\mathbf{d} \cdot \mathbf{E}(z,t) \ , \tag{3}$$

where $\mathbf{d}$ is the electric dipole operator.

Photodissociation results when the energy eigenstates reached by photon absorption are in the continuum. These are defined as eigenstates $|\, E, \mathbf{m}^- \,\rangle$ of the molecular Hamiltonian H_M with continuous energy eigenvalues E, i.e.,

$$[E - H_M]|\, E, \mathbf{m}^- \,\rangle = 0. \tag{4}$$

The index $\mathbf{m}$ designates a collection of additional quantum numbers that may be necessary to completely specify the state. In particular, if we regard the state $|\, E, \mathbf{m}^- \,\rangle$ as representing a collisional or a dissociation process, then $\mathbf{m}$ includes the chemical identity as well as all the *internal* (electronic, vibrational, rotational, etc...) quantum numbers of the molecules that participate in the collision[**4**]. Note that the minus superscript indicates that the eigenstates satisfy the "incoming" boundary conditions. That is, in the distant future these states become the eigenstates of the asymptotic Hamiltonian of the products, denoted $|\, E, \mathbf{m}; 0 \,\rangle$, with the indicated quantum numbers.

In accord with standard perturbation theory applied to photodissociation[**2**], if the molecule is initially in a bound state $|\, E_i \,\rangle$ of energy E_i, then after the pulse is over the portion of the wavepacket excited to a continuous segment of the spectrum is given by

$$|\, \Psi'(t) \,\rangle = \tag{5}$$

$$(2\pi i/\hbar) \sum_{\mathbf{n}} \int dE\ \bar{\epsilon}(\omega_{E,i}) \langle\, E, \mathbf{n}^- \,|\hat{\boldsymbol{\epsilon}} \cdot \mathbf{d}|\, E_i \,\rangle |\, E, \mathbf{n}^- \,\rangle \exp(-iEt/\hbar).$$

where $\bar{\epsilon}(\omega) = \epsilon(\omega) \exp[i\omega z/c]$, with $\omega_{E,i} = (E - E_i)/\hbar$. The quantity $\hat{\boldsymbol{\epsilon}} \cdot \mathbf{d}$ is the projection of the transition-dipole operator along the electric field direction.

The photodissociation probability into the state characterized by $\mathbf{n}$ at energy E, $P_{\mathbf{n}}(E|i)$, is given by the square of $A_{\mathbf{n}}(E|i)$, the photodissociation amplitude for observing the free state $\exp(-iEt/\hbar)|\, E, \mathbf{n}; 0 \,\rangle$ in the long-time limit. That is,

$$P_{\mathbf{n}}(E|i) = |A_{\mathbf{n}}(E|i)|^2\,, \tag{6}$$

with $A_{\mathbf{n}}(E|i)$ defined as

$$A_{\mathbf{n}}(E|i) = \lim_{t \to \infty} \exp(iEt/\hbar) \langle\, E, \mathbf{n}; 0 \,|\Psi(t)\rangle. \tag{7}$$

Because the bound and continuum wavefunctions usually belong to different electronic manifolds, they are orthogonal to one another and the only term that contributes to $A_{\mathbf{n}}(E|i)$ derives from Ψ', the excited part of the wavepacket. It follows from the incoming boundary conditions on $|\, E, \mathbf{n}^- \,\rangle$ that the $t \to \infty$ limit of Eq. (5) can be written as

$$|\, \Psi'(t \to \infty) \,\rangle = \frac{2\pi i}{\hbar} \sum_{\mathbf{n}} \int dE \bar{\epsilon}(\omega_{E,i}) |\, E, \mathbf{n}; 0 \,\rangle \langle\, E, \mathbf{n}^- \,|\hat{\boldsymbol{\epsilon}} \cdot \mathbf{d}|\, E_i \,\rangle \exp(-iEt/\hbar)\ . \tag{8}$$

Using the orthonormality of the $|\, E, \mathbf{n}; 0 \,\rangle$ functions, we obtain from Eq. (7) that

$$A_{\mathbf{n}}(E|i) = \frac{2\pi i}{\hbar} \bar{\epsilon}(\omega_{E,i}) \langle\, E, \mathbf{n}^- \,|\hat{\boldsymbol{\epsilon}} \cdot \mathbf{d}|\, E_i \,\rangle. \tag{9}$$

Note that by using incoming states, we have shown that the coefficient of the state $|\, E, \mathbf{n}^- \,\rangle$ at time $t = 0$ in Eq. (5) is exactly $A_{\mathbf{n}}(E|i)$, the long time photodissociation amplitude. Thus, we obtain the crucial insight that *the probability of obtaining product in the state* $|\, E, \mathbf{n}; 0 \,\rangle$ *is given solely by the probability of preparing the state* $|\, E, \mathbf{n}^- \,\rangle$ *at the time of preparation.*

The traditional scenario of molecular excitation and subsequent system evolution developed in the preceding section, affords little opportunity to control the outcome of molecular events. In order to understand why this is so and how the problem may be overcome[**5**] we note that (even beyond the weak perturbation limit[**3**]) the ratio of probabilities of dissociation into a particular product state at any given time, from a given initial state $|\, E_i \,\rangle$ is given, in accord with Eqs. (6) and (9), by

$$\frac{P_{\mathbf{n}}(E)}{P_{\mathbf{m}}(E)} = \left| \frac{b_{E,\mathbf{n}}(\infty)}{b_{E,\mathbf{m}}(\infty)} \right|^2 = \left| \frac{\langle\, E, \mathbf{n}^- \,|\hat{\boldsymbol{\epsilon}} \cdot \mathbf{d}|\, E_i \,\rangle}{\langle\, E, \mathbf{m}^- \,|\hat{\boldsymbol{\epsilon}} \cdot \mathbf{d}|\, E_i \,\rangle} \right|^2 \quad . \tag{10}$$

Thus, the branching ratios at a fixed energy E, control over which is generally sought, are *independent of the external field(s).* Hence varying the parameters of the external field(s) will have no effect on the asymptotic branching ratios. That is, there is no way we can control the product ratios of the photodissociation event.

This result holds true as long as there is only *one* initial state $|\, E_i \,\rangle$ that is excited to the continuum.

The above argument motivates the idea that the way to control photodissociation is to use more than one initial state, or in greater generality, to use multiple excitation pathways. In this section we demonstrate that such a strategy allows us to actively influence and control which photodissociation product is formed. These ideas, which introduce the notion of "coherent control", hold true for any dynamical process, not just for photodissociation .

2. Weak Field Coherent Control

2.1. Photodissociation from a Superposition State. We introduce the basic principles of coherent control through a series of examples. In particular, we extend the treatment of sub-section 1.1 to the photodissociation of a non-stationary *superposition* of bound states, $|\, \chi(0) \,\rangle = \sum_{j=1}^{N} a_j |\, E_j \,\rangle \exp(-iE_j t/\hbar)$. Numerous experimental techniques can be used to create such a state. Whatever the method of preparation, the amplitude and phase of the coefficients a_j are functions of the experimentally controllable parameters used in creating the superposition.

Repeating the treatment of weak field photodissociation given in sub-section 1.1, but now for an initial superposition state, gives the same result as trivially replacing, in the final result [Eq. (5)], the single initial state $|\, E_i \,\rangle \exp(-iE_i t/\hbar)$ by the superposition $\sum_{j=1}^{N} a_j |\, E_j \,\rangle \exp(-iE_j t/\hbar)$. Thus, at the end of the excitation pulse the system wavefunction at time t is given by,

$$|\, \Psi(t) \,\rangle = \sum_{j=1}^{N} a_j |\, E_j \,\rangle \exp(-iE_j t/\hbar) +$$

$$(2\pi i/\hbar) \sum_{j=1}^{N} a_j \sum_{\mathbf{n}} \int dE\; \bar{\epsilon}(\omega_{E,j}) \langle E, \mathbf{n}^- | \hat{\boldsymbol{\epsilon}} \cdot \mathbf{d} |\, E_j \,\rangle |\, E, \mathbf{n}^- \,\rangle \exp(-iEt/\hbar)\ , \tag{11}$$

where $\omega_{E,j} \equiv (E - E_j)/\hbar$. The probability $P_{\mathbf{n}}(E)$ of being in the final state $|\, E, \mathbf{n}; 0 \,\rangle$ is $P_{\mathbf{n}}(E) = |A_{\mathbf{n}}(E)|^2$, where the probability-amplitude $A_{\mathbf{n}}(E)$ is given by [using Eq. (7)]

$$A_{\mathbf{n}}(E) = \lim_{t \to \infty} \exp(iEt/\hbar) \langle E, \mathbf{n}; 0 |\, \Psi(t) \,\rangle = \frac{2\pi i}{\hbar} \sum_{j=1}^{N} a_j\; \bar{\epsilon}(\omega_{E,j}) \langle E, \mathbf{n}^- | \hat{\boldsymbol{\epsilon}} \cdot \mathbf{d} |\, E_j \,\rangle\ . \tag{12}$$

Of particular interest is the probability of being in a subspace of states, denoted by the label q; that is, in all states $\mathbf{m}$ associated with a fixed q, where $\mathbf{n} = (\mathbf{m}, q)$. Summing over $\mathbf{m}$ we obtain that,

$$P_q(E) = \sum_{\mathbf{m}} P_{\mathbf{m},q}(E) = \sum_{\mathbf{m}} |A_{\mathbf{m},q}(E)|^2. \tag{13}$$

Inserting $A_{\mathbf{m},q}(E)$ from Eq. (12) gives

$$P_q(E) = (2\pi/\hbar)^2 \sum_{i,j=1}^{N} [a_i a_j^* \bar{\epsilon}(\omega_{E,i}) \bar{\epsilon}^*(\omega_{E,j})] \mathrm{d}_q(ji)]\ , \tag{14}$$

where

$$\mathrm{d}_q(ji) = \sum_{\mathbf{m}} \langle E_j \,|\, \hat{\boldsymbol{\epsilon}} \cdot \mathbf{d} \,|\, E, \mathbf{m}, q^- \rangle \langle E, \mathbf{m}, q^- \,|\, \hat{\boldsymbol{\epsilon}} \cdot \mathbf{d} \,|\, E_i \rangle \ . \tag{15}$$

The branching ratio between two channels at energy E, $R_{q,q'}(E)$, which we control below is then,

$$R_{q,q'}(E) = P_q(E)/P_{q'}(E) \ . \tag{16}$$

Consider then the nature of $P_q(E)$ [Eq. (14)]. The diagonal terms ($i = j$) give the standard probability, at energy E, of photodissociation out of a bound state $|\, E_j \,\rangle$ to produce a product in channel q. The off-diagonal terms ($i \neq j$) correspond to interference terms between these photodissociation routes. These interference terms describe the constructive enhancement, or destructive cancellation, of product formation in subspace q. Equation (14) is important *in practice* because the interference terms have coefficients $[a_i a_j^* \bar{\epsilon}(\omega_{E,i}) \bar{\epsilon}^*(\omega_{E,j})]$ whose magnitude and sign depend upon *experimentally controllable* parameters. Thus the experimentalist can manipulate laboratory parameters and, in doing so, alter the interference term and hence control the reaction product yield. This control approach can be extended to the domain of moderately strong fields[**6**].

Equation (14) displays an important feature. That is, the entire control map, i.e., $P_q(E)$ or $R_{q,q'}(E)$ as a function of the control parameters, is a function of very few molecular parameters, i.e., the $\mathrm{d}_q(ji)$. As a consequence, the experimentalist need only determine these few parameters in order to produce the entire control map. This statement constitutes the weak field version of "Adaptive Feedback Control" (see, e.g. [**7**]-[**12**]). In the general strong field regime, a numerical non-linear search procedure must be performed to achieve a desired optimization. However, in the weak-field regime, because of the simple bilinear dependence of each $P_q(E)$ on the $a_j \bar{\epsilon}(\omega_{E,j})$ experimental parameters, we need only carry out N^2 measurements for each arrangement channel to determine all the $d_q(ji)$ coefficients. Once these coefficients are known, the bilinear $P_q(E)$ function can be analytically interpolated to give any desired branching ratio between, and including, the extrema of $R_{q,q'}(E)$.

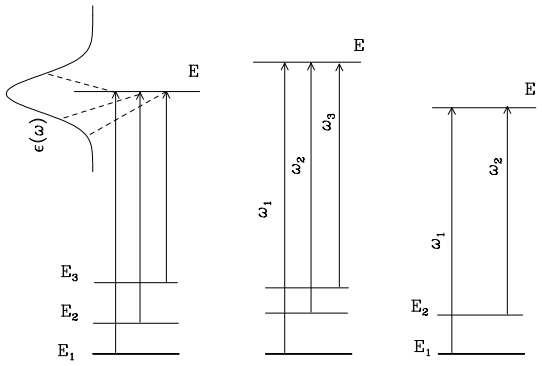

FIGURE 1. Photodissociation of a superposition of N levels using (a) a pulsed light source ($N = 3$ is shown); (b) N cw lasers ($N = 3$ is shown) , and (c) $N = 2$ with two cw lasers.

2.2. Bichromatic Control. Experimentally attaining control via Eq. (14) requires a light source containing N frequencies $\omega_i, (i = 1...N)$. Both pulsed excitation with a source whose frequency width encompasses these frequencies, as well as excitation with N Continuous Wave (cw) lasers of frequencies $\omega_i = \omega_{E,i}$, $(i = 1...N)$ are possible approaches, as depicted in Fig. 1. Here we focus on $N = 2$, i.e., the effect of two cw lasers on a system in a superposition of two states [Fig. 1c], a scenario termed "bichromatic control".

Consider then two parallel cw fields of frequencies ω_1 and ω_2 incident on a molecule. The light-molecule interaction potential [Eq. (3)] is then

$$H_{MR}(t) = -\sum_{i=1}^{2} 2\mathbf{d}\cdot\hat{\epsilon}\ \mathrm{R}_e[\bar{\epsilon}(\omega_i)\exp(-i\omega_i t)]\ . \tag{17}$$

Tuning the ω_1 and ω_2 frequencies such that, $\omega_2 - \omega_1 = (E_1 - E_2)/\hbar$, we have that $P_q(E)$ of Eq. (14), at energy $E = E_1 + \hbar\omega_1 = E_2 + \hbar\omega_2$, has only two contributions, corresponding to the excitations shown in Fig. 1c. The quantities $P_q(E = E_1 + \hbar\omega_1)$ and $R_{q,q'}(E)$ are therefore given by[**13, 14**]

$$\left(\frac{\hbar}{2\pi}\right)^2 P_q(E = E_1 + \hbar\omega_1) =$$

$$|a_1|^2|\bar{\epsilon}(\omega_1)|^2\mathrm{d}_q(11) + |a_2|^2|\bar{\epsilon}(\omega_2)|^2\mathrm{d}_q(22) + 2\ \mathrm{R}_e[a_1a_2^*\bar{\epsilon}(\omega_1)\bar{\epsilon}^*(\omega_2)\mathrm{d}_q(12)]\ , \tag{18}$$

$$R_{q,q'}(E) = \frac{|\mathrm{d}_q(11)| + x^2|\mathrm{d}_q(22)| + 2x\cos(\theta_1 - \theta_2 + \alpha_q(12))|\mathrm{d}_q(12)|}{|\mathrm{d}_{q'}(11)| + x^2|\mathrm{d}_{q'}(22)| + 2x\cos(\theta_1 - \theta_2 + \alpha_{q'}(12))|\mathrm{d}_{q'}(12)|}\ , \tag{19}$$

where $\alpha_q(ij)$ and θ_j are defined via

$$\begin{aligned} \mathrm{d}_q(ij) &= |\mathrm{d}_q(ij)|\exp(i\alpha_q(ij))\ ,\ x = \frac{|\bar{\epsilon}(\omega_2)a_2|}{|\bar{\epsilon}(\omega_1)a_1|}\ , \\ \tan\theta_j &= \frac{\mathrm{Im}[\bar{\epsilon}(\omega_j)a_j]}{\mathrm{Re}[\bar{\epsilon}(\omega_j)a_j]}\ . \end{aligned} \tag{20}$$

For convenience we have introduced the control variables $\Delta\theta = \theta_1 - \theta_2$ and $s = x^2/[x^2 + 1]$. The range $0 \le s \le 1$ covers all possible values of relative laser intensities. Varying $\Delta\theta$ or s, changes the interference term and thus gives us control over the dissociation probabilities. These changes may be accomplished either by varying the coefficients of the initial superposition state, $\{a_j\}$, or by changing the intensity and relative phases of the dissociation lasers. Note, in particular, that varying $\Delta\theta$ corresponds to just varying a phase. The dependence of the yield on $\Delta\theta$ hence emphasizes the quantum-interference-based nature of the control.

As an example of this approach we consider control over the relative probability of forming $^2P_{3/2}$ vs. $^2P_{1/2}$ atomic iodine, denoted I and I*, in the dissociation of methyl iodide in the regime of 266 nm,

$$\mathrm{CH_3} + \mathrm{I}^*(^2P_{1/2}) \leftarrow \mathrm{CH_3I} \rightarrow \mathrm{CH_3} + \mathrm{I}(^2P_{3/2})\ . \tag{21}$$

This reaction is an example of electronic branching of photodissociation products. The results reported below are for a non-rotating two-dimensional model[**15**] in which the H_3 center-of-mass, the C and the I atoms are assumed to lie on a straight line.

Typical results for the control of the I vs. I* channel are shown in Fig. 2, as contour plots of the yield of CH_3 + I as a function of the control parameters. Two

cases are shown: photodissociation out of the two superposition states $|\chi(0)\rangle = a_1|E_1\rangle + a_2|E_2\rangle$ (Figure 2a) and $|\chi(0)\rangle = a_1|E_1\rangle + a_3|E_3\rangle$ (Figure 2b). Here $|E_1\rangle$ is the ground state and $|E_2\rangle$ and $|E_3\rangle$ correspond to states with one and two quanta of excitation in the C-I bond. The results show a large range of possible control. For example, the yield changes in Fig. 2b from 30% to 70% as one varies s at small $\theta_1 - \theta_2$. In addition, a comparison of the two figures shows that the topology of the control plot depends strongly on the states that comprise the superposition state.

2.2.1. *Energy Averaging and Satellite Contributions.* In general, experiments measure energy averaged quantities such as

$$P_q = \int dE\ P_q(E)\ ,\ R_{q,q'} = P_q/P_{q'}\ , \tag{22}$$

since products are not distinguished on the basis of total energy. As such, it is necessary to compute photodissociation to all energies. For the case considered above, two states irradiated with two cw fields of frequencies ω_1 and ω_2, $P_q(E)$ [Eq. (14)] is nonzero at three energies:
$E = E_1 + \hbar\omega_1 = E_2 + \hbar\omega_2$, $E' = E_1 + \hbar\omega_2$ and $E'' = E_2 + \hbar\omega_1$.

The contribution from the first of these energies $P_q(E = E_1 + \hbar\omega_1)$ is given in Eq. (18) and shown on the left hand side of Fig. 3. The remaining contributions, shown on the right hand side of Fig. 3, are

$$\begin{aligned} P_q(E' = E_1 + \hbar\omega_2) &= (\frac{2\pi}{\hbar})^2 |a_1\bar{\epsilon}(\omega_2)|^2 \mathrm{d}_q(11)\ , \\ P_q(E'' = E_2 + \hbar\omega_1) &= (\frac{2\pi}{\hbar})^2 |a_1\bar{\epsilon}(\omega_1)|^2 \mathrm{d}_q(22)\ . \end{aligned} \tag{23}$$

Thus, the overall P_q for $N = 2$ is given by

$$P_q = P_q(E = E_1 + \hbar\omega_1) + P_q(E' = E_1 + \hbar\omega_2) + P_q(E'' = E_2 + \hbar\omega_1)\ . \tag{24}$$

The latter two terms correspond to traditional photodissociation terms without associated interference contributions and provide *uncontrollable* photodissociation terms that we call "satellites". In this, and all coherent control scenarios discussed below, it is important to attempt to reduce the relative magnitude of the satellite terms in order to increase overall controllability.

We make the general observation that interference between terms of different energies contain oscillatory $\exp[i(E_1 - E_2)t/\hbar]$ terms that average out to zero with time. (This is not to say that the oscillatory interference term can not be put to good use. See, for example, a proposal for generating THz radiation [**16**] using such oscillatory terms and a related experiment[**17**]).

3. The Principle of Coherent Control

Control of the type discussed above, in which quantum interference effects are used to constructively or destructively alter product properties, is called coherent control. Photodissociation of a superposition state, the scenario described above, will be seen to be just one particular implementation of a general principle of coherent control: i.e., that *coherently driving a state with phase coherence through multiple, coherent, indistinguishable, optical excitation routes to the same final state allows for the possibility of control*. This procedure has a well-known analogy, the

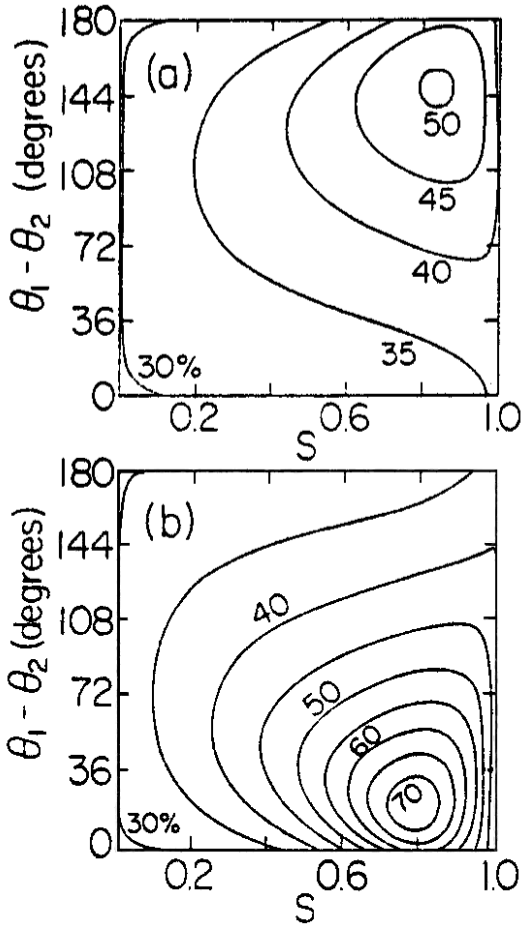

FIGURE 2. Contour plot of the yield of CH_3 +I from the photodissociation of CH_3I from a superposition of states at $\omega_1 = 37593.9$ cm^{-1}. (a) $|\chi(0)\rangle = a_1|E_1\rangle + a_2|E_2\rangle$, (b) $|\chi(0)\rangle = a_1|E_1\rangle + a_3|E_3\rangle$. Taken from Fig. 1, Ref. [**13**].

interference between paths as a beam of either particles or of light passes through a double slit. In that case interference between two coherent beams leads to spatial patterns of enhanced or reduced probabilities on an observation screen. In the case of coherent control the overall coherence of a pure state plus laser source

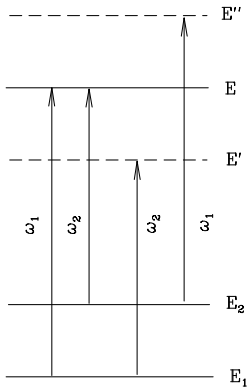

FIGURE 3. Contributions for two levels photodissociated by two frequencies. The interference terms correspond to total energy $= E$. The satellite terms correspond to total energies $= E'$ and E''.

allows for the constructive or destructive manipulation of probabilities in product channels. Active control results because the excitation process explicitly imparts experimentally controllable phase and amplitude information to the molecule.

As mentioned above, in general control can only arise from energetically degenerate states. Another way of seeing this is to note that products of states of different energies E and E' appearing in the square of the wavepacket of Eq. (11) cannot contribute to any measurement where the total energy is resolved. Such a measurement, which filters out all the wavepacket components save those belonging to a given value of E, eliminates all the $E \neq E'$ products. Alternatively, we note that two states of different energy are in principle distinguishable. Hence they can not interfere with one another.

Numerous other scenarios can be designed that rely upon the essential coherent control principle. Examples include N photon vs. M photon routes and pump-dump scenarios reliant upon pulsed laser excitation. In the former case, situations where the N and M excitations are of different parity allow for interesting symmetry breaking situations, including the ability to exercise control over chirality[**18, 19, 20**].

4. Interference Between N-Photon and M-Photon Routes

Another important example of coherent control introduces the possibility of quantum interference arising through competitive optical routes in the excitation of a single bound state to an energy E. Specifically, we consider the photodissociation of a single state via two pathways, an N photon and an M photon dissociation route. The N vs. M scenarios are of two types, N and M of the same parity (i.e., both N and M odd or both even) or of opposite parity. The latter allows for control over the differential photodissociation cross sections (i.e., scattering into different angles), or control of the integral cross-sections of systems lacking an inversion center ("chiral" systems), whereas the former allows for control over both the integral and differential cross sections. For simplicity we focus on the two lowest order cases $(N, M) =$(1,2) and $(N, M) = (1, 3)$.

4.1. One vs. Three Photon Interference. Consider[**21**] a molecule initially in state $|\, E_i \,\rangle$ subjected to two co-propagating cw fields of frequencies ω_1 and ω_3, with $\omega_3 = 3\omega_1$. The interaction potential is given by

$$H_{MR}(t) = -2\mathbf{d}\cdot\ \mathrm{R}_e\left[\hat{\boldsymbol{\epsilon}}_3\bar{\epsilon}_3\exp(-i\omega_3 t) + \hat{\boldsymbol{\epsilon}}_1\bar{\epsilon}_1\exp(-i\omega_1 t)\right]\ , \tag{25}$$

where $\bar{\epsilon}_i = \bar{\epsilon}(\omega_i)$.

We assume the following physics: (a) the dipole transitions within electronic states are negligible compared to those between electronic states; (b) the fields are sufficiently weak to allow the use of perturbation theory, and (c) $E_i + 2\hbar\omega_1$ is below the dissociation threshold, with dissociation occurring from the excited electronic state. The lowest order perturbation theory expression for the one-photon or three-photon dissociation amplitude $A_{\mathbf{m},q}(E = E_i + \hbar\omega_3)$ is

$$A_{\mathbf{m},q}(E = E_i + \hbar\omega_3) = (\frac{2\pi i}{\hbar})\times \tag{26}$$

$$\left[\delta(\omega_3 - \omega_{E,i})\bar{\epsilon}_3\ \langle\, E, \mathbf{m}, q^- \,|\, \mathrm{d}_{e,g} \,|\, E_i \,\rangle + \delta(3\omega_1 - \omega_{E,i})\bar{\epsilon}_1^3\ \langle\, E, \mathbf{m}, q^- \,|\, T_{e,g} \,|\, E_i \,\rangle\right]\ ,$$

where, $T_{e,g}$ is the 3-photon transition operator, given in third order perturbation theory as

$$T_{e,g} = \sum_{e'\,e''} \mathrm{d}_{e,e'}(E_i - H_{e'} + 2\hbar\omega_1)^{-1}\mathrm{d}_{e',e''}(E_i - H_{e''} + \hbar\omega_1)^{-1}\mathrm{d}_{e'',g}\ . \tag{27}$$

The probability to produce fragments q at a fixed energy E is therefore

$$P_q(E) = \sum_{\mathbf{m}} |A_{\mathbf{m},q}(E_i + \hbar\omega_3)|^2 = P_q^{(1)}(E) + P_q^{(3)}(E) + P_q^{(13)}(E)\ , \tag{28}$$

where the one photon photodissociation probability is

$$P_q^{(1)}(E) = (\frac{2\pi}{\hbar})^2|\bar{\epsilon}_3|^2 \sum_{\mathbf{m}} |\langle\, E, \mathbf{m}, q^- \,|\, \mathrm{d}_{e,g} \,|\, E_i \,\rangle|^2\ , \tag{29}$$

the three-photon dissociation probability is

$$P_q^{(3)}(E) = (\frac{2\pi}{\hbar})^2|\bar{\epsilon}_1|^6 \sum_{\mathbf{m}} |\langle\, E, \mathbf{m}, q^- \,|\, T_{e,g} \,|\, E_i \,\rangle|^2\ , \tag{30}$$

and the one-photon three-photon interference term is

$$P_q^{(13)}(E) = (\frac{2\pi}{\hbar})^2 \left[\bar{\epsilon}_3\ \bar{\epsilon}_1^3\ \sum_{\mathbf{m}} \langle\, E_i \,|\, T_{g,e} \,|\, E, \mathbf{m}, q^- \,\rangle \langle\, E, \mathbf{m}, q^- \,|\, \mathrm{d}_{e,g} \,|\, E_i \,\rangle + c.c.\right]\ . \tag{31}$$

As in our discussion of the photodissociation of a superposition state [section 2.1] we define a "molecular" interference-amplitude $|F_q^{(13)}|$ and a "molecular" phase $\alpha_q(13)$ as

$$|F_q(13)|\exp[i\alpha_q(13)] = \sum_{\mathbf{m}} \langle\, E_i \,|\, T_{g,e} \,|\, E, \mathbf{m}, q^- \,\rangle \langle\, E, \mathbf{m}, q^- \,|\, \mathrm{d}_{e,g} \,|\, E_i \,\rangle\ . \tag{32}$$

Recognizing that $\bar{\epsilon}_i$ is a complex number, $\bar{\epsilon}_i = |\bar{\epsilon}_i|e^{i\phi_i}$ we can write the above interference term as

$$P_q^{(13)}(E) = -2(\frac{2\pi}{\hbar})^2|\bar{\epsilon}_3\bar{\epsilon}_1^3|\cos(\phi_3 - 3\phi_1 + \alpha_q(13)|F_q(13)|\ . \tag{33}$$

The branching ratio $R_{qq'}(E)$ for channels q and q', (see Eq. (16)) can now be written as

$$R_{qq'}(E) = \frac{F_q(11) - 2x\cos[\phi_3 - 3\phi_1 + \alpha_q(13)]\epsilon_0^2|F_q(13)| + x^2\epsilon_0^4 F_q(33)}{F_{q'}(11) - 2x\cos[\phi_3 - 3\phi_1 + \alpha_{q'}(13)]\epsilon_0^2|F_{q'}(13)| + x^2\epsilon_0^4 F_{q'}(33)} \ . \tag{34}$$

where

$$F_q(11) = (\frac{\hbar}{\pi|\bar{\epsilon}_3|})^2 P_q^{(1)}(E) \ ; \ F_q(33) = (\frac{\hbar}{\pi|\bar{\epsilon}_1|^3})^2 P_q^{(3)}(E) \ ;$$

$$\text{and } x = \frac{|\bar{\epsilon}_1|^3}{\epsilon_0^2|\bar{\epsilon}_3|} \ , \tag{35}$$

where ϵ_0 is defined as a single unit of electric field; x is therefore a dimensionless parameter.

The numerator and denominator of Eq. (34) each display the canonical form for coherent control, i.e., a form similar to Eq. (19) in which there are independent contributions from more than one route, modulated by an interference term. Since the interference term is controllable through variation of the (x and $\phi_3 - 3\phi_1$) laboratory parameters, so too is the branching ratio $R_{qq'}(E)$. Thus, the principle upon which this control scenario is based is the same as that in Section 2.1 but the interference is introduced in an entirely different way.

The 3-photon vs. 1-photon scenario has been experimentally realized by Elliott *et al* in atoms[**22**], and by Gordon and coworkers [**23**]–[**27**] in a series of experiments on HCl and CO. For example, Gordon demonstrated control over the production of different channels in the $HI^+ \leftarrow HI \rightarrow H+I$ case[**26, 27**]. The experimental results, shown in Fig. 4, are highly significant since the modulations in the I^+ signal are seen to be *out of phase* with those of the HI^+ signal. Thus, control over different reaction products has been demonstrated. That is, by changing $\phi_3 - 3\phi_1$, the phase difference between the ω_3 and the ω_1 laser fields, through the change in the pressure of the H_2 gas in the tuning cell, different I^+/HI^+ ratios are attained.

The quantitative nature of the observed control depends upon the values of $F_q^{(13)}$ and the "molecular phase", α_q. In particular, the value of $\alpha_q - \alpha_{q'}$ dictates the shift between the peaks in $P_q(E)$ and $P_{q'}(E)$. For example, a molecular case where $\alpha_q - \alpha_{q'} \approx 0$ (e.g., in the $H_2S^+ \leftarrow H_2S \rightarrow H+HS$ case discussed above) shows less discrimination between channels than does a molecular case where $\alpha_q - \alpha_{q'} = \pi$. Hence the relationship between the nature of the dynamics and the α_q values is of interest, a topic studied in detail by Gordon, Seideman and coworkers[**28**].

The above results show that it is possible to control the integral cross section into channel q via one photon vs. three photon absorption. A similar result obtains for any N photon vs. M photon absorption scenario where N and M are of the same parity. In addition, these scenarios allow for control over differential cross sections as well. To see this, consider rewriting Eqs. (29) - (32) so that it applies to the probability of observing the product in channel q, but at a fixed scattering angle. Then the sum over the channel indices $\mathbf{m}$ no longer includes an integral over scattering angles. The resultant cross term $P^{(13)}$ is nonzero so that varying properties of the lasers will indeed alter the differential cross section into channel q.

This introduction makes clear that quantum interference provides a central means for the quantum control of molecular processes. As noted above, this has

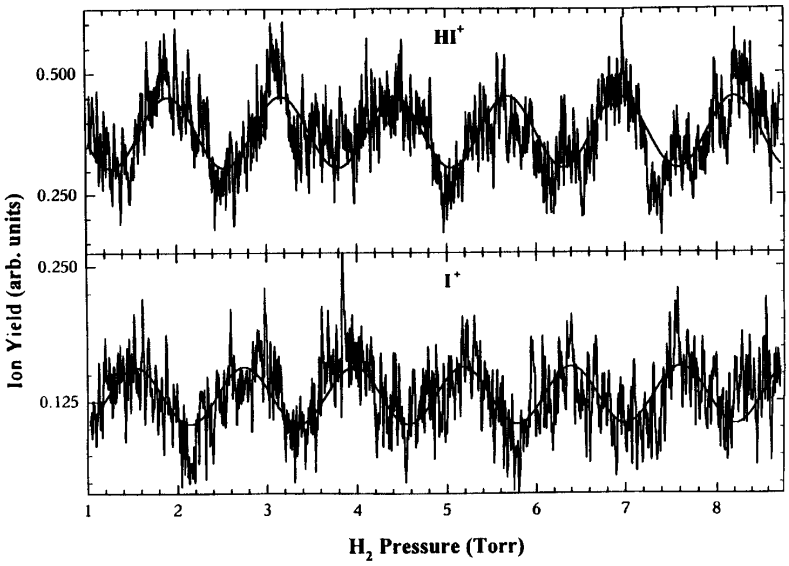

FIGURE 4. Modulation of the HI^+ and I^+ signals as a function of the difference between the one- and three-photon phases (proportional to the H_2 pressure in the cell used to phase shift the beams). Taken from Fig. 3, Ref.[**26**].

been applied to a wealth of processes, providing deep insights into the mechanisms for control.

5. Large Molecule Control

Consider now the problem of simulating coherent-control in a large molecular system. In this case, unlike the situation above, interest is generally in controlling the dynamics of a subcomponent of the system, e.g the photo-induced proton transfer motion in the molecule 2-(2'-hydroxyphenyl)-oxazole (denoted HPO through out this paper) shown in Figure 5. In such an instance one might try to control the motion of the proton between the keto and enol forms of the molecule. To do so using quantum interference requires the maintenance of quantum coherence throughout the process. However, it is well known that a quantum subsystem, in interaction with the total system, undergoes decoherence, i.e. the loss of the coherence that need be maintained in order to achieve control. Hence, the study summarized below aimed to demonstrate that control was indeed possible in the presence of decoherence[**29, 30**] induced by coupling to the molecular background. To do so required the development of a new semiclassical approach to the molecular dynamics, also summarized below, since quantum computations are intractable.

We consider control over proton transfer in HPO using the bichromatic control scenario discussed above. For this finite time computation it is convenient to

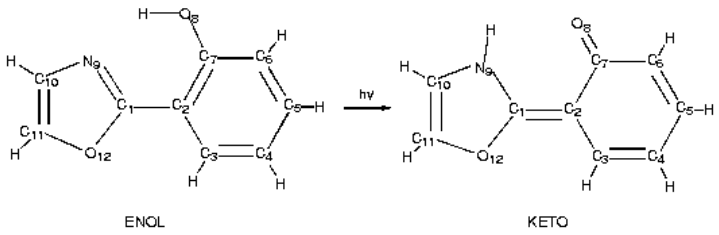

FIGURE 5. Molecular structural diagram describing the excited state intramolecular proton transfer reaction in 2-(2'-hydroxyphenyl)-oxazole. Taken from Fig. 2, Ref. [**31**].

introduce a slightly different notation from that above and to ignore the spatial dependence of the electric field. Here the molecule is initially prepared in a coherent superposition state,

$$| \Psi(0)\rangle = c_1 \mid 1\rangle + c_2 \mid 2\rangle, \tag{36}$$

where $\mid i\rangle$ is a bound nuclear eigenstate of energy E_i. The system is subsequently photoexcited by two monochromatic laser pulses with a total electric field $\boldsymbol{\epsilon}(t)$

$$\boldsymbol{\epsilon}(t) = F_1(t-t_1)\boldsymbol{\epsilon}_1 e^{-i(\omega_1 t+\theta_1)} + F_2(t-t_2)\boldsymbol{\epsilon}_2\, e^{-i(\omega_2 t+\theta_2)} + \text{c.c}, \tag{37}$$

where $\boldsymbol{\epsilon}_j = \epsilon_j \hat{\boldsymbol{\epsilon}},\ j = 1,2$ are time independent real vectors, and c.c. denotes the complex conjugate of the preceding terms. The functions F_j in Eq. (37), describe the pulse shapes, and θ_j are the phases of the two pulses.

Unlike the photodissociation case above, here we are interested in the time dependence of the reactant population. The time-dependent reactant population $P(t)$ can be computed as follows:

$$P(t) \equiv \langle \Psi(t) \mid R \mid \Psi(t)\rangle, \tag{38}$$

R is a function of the system coordinates that is one only when the system is in the reactant side of a dividing surface in configuration space and $\mid \Psi(t)\rangle$ is the system wavefunction at time t.

Assuming that the laser field is sufficiently weak to allow the use of first order perturbation theory, we obtain the time evolved wave function $\mid \Psi(t)\rangle$ as

$$\begin{aligned} | \Psi(t)\rangle = -\frac{i}{\hbar}\sum_{j=1}^{2} c_j \int_{-\infty}^{t} dt' \,[\sum_{k=1}^{2} \epsilon_k e^{-i[(E_j+\hbar\omega_k)t'/\hbar+\theta_k]} \\ \times F_k(t'-t_k)] e^{-i\hat{H}(t-t')/\hbar}\hat{\boldsymbol{\epsilon}}\cdot\mathbf{d} \mid j\rangle. \end{aligned} \tag{39}$$

where $\hat{H}$ is the Hamiltonian on the excited electronic surface, and where only the near resonant terms have been retained (the rotating wave approximation). Substituting Eq. (39) into Eq. (38), we obtain the time dependent reactant population

in the weak field limit

(40)

$$P(t) = \hbar^{-2} \int_{-\infty}^{t} dt' \int_{-\infty}^{t} dt'' \sum_{j,j'=1}^{2} c_j c_{j'}^* \langle j' \mid \hat{\boldsymbol{\epsilon}} \cdot \mathbf{d} e^{i\hat{H}(t-t'')/\hbar} R e^{-i\hat{H}(t-t')/\hbar} \hat{\boldsymbol{\epsilon}} \cdot \mathbf{d} \mid j \rangle$$
$$\times e^{i(E_{j'}t'' - E_j t')/\hbar} \epsilon_1^2 (F_1(t'-t_1)F_1(t''-t_1)e^{i\omega_1(t''-t')} + F_2(t'-t_2)F_2(t''-t_2)x^2$$
$$\times e^{i\omega_2(t''-t')}) + F_2(t'-t_2)F_1(t''-t_1)e^{i[(\omega_1 t'' - \omega_2 t') + \Theta]} + F_1(t'-t_1)F_2(t''-t_2)$$
$$\times x\, e^{i[(\omega_2 t'' - \omega_1 t') - \Theta]}],$$

as a function of the laser controllable parameters $x = \epsilon_2/\epsilon_1$, and $\Theta = \theta_1 - \theta_2$. Note that Eq. (40) contains terms in $|c_j|^2$ corresponding to direct contributions, as well as terms in $c_j c_j'$ that correspond to interference terms. Hence, by altering the c_j we can control the interference term, and hence the dynamics.

To compute the control requires the exact quantum propagation of the system, a computational task that becomes daunting, if not intractable, for systems with more than six degrees of freedom (e.g., a molecule with four atoms). For this reason we turn to semiclassical methods.

6. Semiclassical Initial Value Representation

In an effort to develop an *approximate* method of useful reliability for the description of quantum mechanical interferences in systems with many degrees of freedom, we replace the time evolution operators, in Eq. (40), by the coherent state expression in the initial value representation (IVR)[**32**]. That is,

$$e^{-i\hat{H}t/\hbar} = (2\pi\hbar)^{-N} \int d\mathbf{p}_0 \int d\mathbf{q}_0 \; e^{iS_t(\mathbf{p}_0,\mathbf{q}_0)/\hbar} C_t(\mathbf{p}_0,\mathbf{q}_0) \; \mid g_{\mathbf{q}_t,\mathbf{p}_t} \rangle\langle g_{\mathbf{q}_0,\mathbf{p}_0} \mid, \tag{41}$$

where $\mid g_{\mathbf{q},\mathbf{p}} \rangle$ is a coherent state. The integration variables $(\mathbf{p}_0, \mathbf{q}_0)$ in Eq. (41) are the initial conditions for classical trajectories and $\mathbf{q}_t \equiv \mathbf{q}_t(\mathbf{p_0}, \mathbf{q_0})$ and $\mathbf{p}_t \equiv \mathbf{p}_t(\mathbf{p_0}, \mathbf{q_0})$ are the time-evolved nuclear coordinates and momenta. The classical action $S_t(\mathbf{p_0}, \mathbf{q_0})$ along this trajectory is obtained by integrating the equation:

$$\dot{S}_t = \mathbf{p}_t \cdot \dot{\mathbf{q}}_t - H(\mathbf{p}_t, \mathbf{q}_t), \tag{42}$$

along with Hamilton's equations of motion for $\mathbf{p}_t$ and $\mathbf{q}_t$. Here, $H(\mathbf{q}, \mathbf{p})$ is the full-dimensional model Hamiltonian [**33**] that explicitly describes the motion of all degrees of freedom in the system. The pre-exponential factor $C_t(\mathbf{p_0}, \mathbf{q_0})$, introduced in Eq. (41), involves the monodromy matrix elements that are propagated in accord with reference [**33**].

Substituting Eq. (41) into Eq. (40) gives the semiclassical IVR for $P(t)$

$$P(t) = \hbar^{-2} (2\pi\hbar)^{-2N} \int d\mathbf{p}_0 \int d\mathbf{q}_0 \int d\mathbf{p'}_0 \int d\mathbf{q'}_0 \int_{-\infty}^{t} dt' \int_{-\infty}^{t} dt'' \sum_{j,j'} c_j c_{j'}^*$$
$$\times e^{i(S_{t-t'}(\mathbf{p}_0,\mathbf{q}_0) - S_{t-t''}(\mathbf{p'}_0,\mathbf{q'}_0))/\hbar} C_{t-t'}(\mathbf{p}_0,\mathbf{q}_0) C^*_{t-t''}(\mathbf{p'}_0,\mathbf{q'}_0) \langle j' \mid \mathbf{p'}_0, \mathbf{q'}_0 \rangle$$
$$\times \langle \mathbf{p'}_{\mathbf{t-t''}}, \mathbf{q'}_{t-t''} \mid R \mid \mathbf{p}_{t-t'}, \mathbf{q}_{t-t'} \rangle \langle \mathbf{p}_0, \mathbf{q}_0 \mid j \rangle e^{i(E_{j'}t'' - E_j t')/\hbar} \epsilon_1^2 [F_1(t'-t_1)$$
$$\times F_1(t''-t_1) e^{i\omega_1(t''-t')} + F_2(t'-t_2)F_2(t''-t_2)x^2 e^{i\omega_2(t''-t')} + F_2(t'-t_2)$$
$$\times F_1(t''-t_1) x e^{i[(\omega_1 t'' - \omega_2 t') + \Theta]} + F_1(t'-t_1)F_2(t''-t_2) x e^{i[(\omega_2 t'' - \omega_1 t') - \Theta]}]. \tag{43}$$

This time dependent semiclassical formulation extends the usual bichromatic coherent-control scenario to simulate control at finite times after photoexcitation of the system. Applicable to the bound state problem, it has a number of computational advantages relative to the continuum problem. First, there is no need to solve the complete state-to-state quantum mechanical reactive scattering problem; second, the approach provides a "direct" method for computing bichromatic control insofar as it computes $P(t)$, as a function of the pulse phases and intensities, without having to store or compute any other intermediate quantities; third, the method is applicable to systems with many degrees of freedom.

7. Numerical Aspects of the Semiclassical Approach

Semiclassical implementations of problems with this number of atoms are still in their early stages of development[**34**]. Most recently, we have demonstrated, with applications to collinear polyatomic photodissociation[**35**] and non-adiabatic ICN photodissociation[**36**], that the IVR method does provides an excellent approximation to the exact quantum results for controlled photodissociation. Encouraged by these results, we applied this method to the HPO discussed herein[**31**]. The extension to large molecules and to time dependent bound state dynamics introduces a number of computational issues that are discussed in this section.

7.1. Monte Carlo Sampling. In principle, the most efficient implementation of Eq. (43) is one that samples initial conditions for $(\mathbf{p}_0, \mathbf{q}_0)$, $(\mathbf{p'}_0, \mathbf{q'}_0)$ and (t', t'') for pairs of trajectories that propagate forward in time, and contribute at each time t according to the integrand of Eq. (43). In practice, however, such an approach converges extremely slowly for systems with many degrees of freedom, even when implemented according to a stratified adaptive Monte Carlo technique. We, therefore, change the integration variables $(\mathbf{p'}_0, \mathbf{q'}_0)$ to $(\mathbf{p'}_{t-t''}, \mathbf{q'}_{t-t''})$ and we optimize the convergence for each specific time t by sampling $(\mathbf{p'}_{t-t''}, \mathbf{q'}_{t-t''})$ according to a defensive importance sampling technique [**37**].

Trajectories are initialized through MC sampling of coordinates and momenta $(\mathbf{p}_0, \mathbf{q}_0)$ according to the localized phase space distributions $|\langle \mathbf{p}_0, \mathbf{q}_0 \mid \Psi_0 \rangle|^2$. The partial contribution of a single trajectory to $P(t)$ requires forward propagation from the initial phase point $(\mathbf{p}_0, \mathbf{q}_0)$ to the resulting phase point $(\mathbf{p}_{t-t'}, \mathbf{q}_{t-t'})$. At this time the trajectory undergoes a stochastic hop, $(\mathbf{p}_{t-t'}, \mathbf{q}_{t-t'}) \rightarrow (\mathbf{p'}_{t-t''}, \mathbf{q'}_{t-t''})$, and then evolves backward from $(\mathbf{p'}_{t-t''}, \mathbf{q'}_{t-t''})$ to the resulting phase point $(\mathbf{p'}_0, \mathbf{q'}_0)$ at time 0.

The sampling function for coordinates and momenta $(\mathbf{p'}_{t-t''}, \mathbf{q'}_{t-t''})$ is defined in terms of the overlap of the coherent states as

$$
\begin{aligned}
f(\mathbf{p'}_{t-t''}, \mathbf{q'}_{t-t''}) &= (1-\beta) \prod_{j=1}^{N} \sqrt{\frac{\delta}{\pi}} e^{-\delta (p_{t-t'}(j) - p'_{t-t''}(j))^2} \\
&\times e^{-\delta (q_{t-t'}(j) - q'_{t-t''}(j))^2} + \beta \prod_{j=1}^{N} |\langle p'_{t-t''}, q'_{t-t''} \mid p_{t-t'}, q_{t-t'} \rangle|,
\end{aligned} \tag{44}
$$

where δ is a constant parameter and the convergence rate β is adjusted according to the dimensionality of the problem. The role of the first term in Eq. (44) is to provide a localized distribution that samples coordinates and momenta $(\mathbf{p'}_{t-t''}, \mathbf{q'}_{t-t''})$

sufficiently close to $(\mathbf{p}_{t-t'}, \mathbf{q}_{t-t'})$ as to have partial cancellation of the phase in the integrand. The second term is a broad distribution that is essential to provide an upper bound to the variance when the first term is much smaller than the value of the integrand.

It was found that chaotic trajectories cause a serious deterioration in the accuracy and convergence of the calculations. Contributions to the integrand in Eq. (43) from individual trajectories of this kind become exponentially large with time since magnitudes of the stability matrix elements, appearing in the pre-exponential factors $C_t(\mathbf{p}_0, \mathbf{q}_0)$, increase on the average as $\exp(\lambda\ t)$ where λ is the Lyapunov number [**38, 39**]. Consequently, even a few chaotic trajectories can dominate the rate of convergence in the semiclassical calculation. In general, however, the contribution from various chaotic trajectories tend to mutually cancel, presumably as a result of rapid variations in the phases of these contributions. We, therefore, implement a simple procedure [**39**] that removes the trajectories that are highly unstable. Specifically, trajectories in which $\mid C_t(\mathbf{p}_0, \mathbf{q}_0) \mid$ exceeds a cutoff value of 2×10^4 are terminated at that time and their contribution at longer times is set to zero.

7.2. Forward-Backward Time Average. The efficiency of the method, as implemented here relies on the partial cancellation of phases that results from the forward-backward aspect of the calculation, where the product of the two time evolution operators in Eq. (40) is treated as *one* evolution operator [**33**]. This phase cancellation effect is combined with the "smoothing" effect associated with the *time average* over nuclear motion, introduced by the time integrals in Eq. (43). These time integrals are computed via Monte Carlo sampling of propagation times $(t - t')$ and $(t - t'')$, in accord with the distribution functions introduced by the intensity profiles F_1 and F_2, respectively. Thus, the presence of a pulse of finite (as opposed to delta function) duration significantly aids in the convergence of the semiclassical method.

7.3. Approximate Prefactor. The pre-exponential factor $C_t(\mathbf{p_0}, \mathbf{q_0})$, in Eq. (43), is computed by the approximate version of the semiclassical initial value representation method developed in reference [**40**], as implemented in reference [**33**]. The method is specifically designed to avoid the computational bottleneck for applications of the SC-IVR to large molecular systems, which is caused by the calculation of the monodromy matrix elements involved in the pre-exponential factor of the semiclassical amplitude.

7.4. Computational Results. Results of this control computation are given below. For example, Fig. 6 shows a contour plot of the percentage enol (i.e. the reactant) form at 100 fs after photoexcitation of the system. The coherent-control map [Fig. 6] indicates that the percentage reactant drastically changes as a function of the relative pulse laser parameter Θ. That is, there is a broad range of yield control over an extended range of S. Maximum control is attained in the $0.25 < S < 0.55$ range, where the production of the keto tautomer can be varied from more than 20 % to less than 80 %, by varying Θ from 0^o to $\sim 210^o$. Note that these large changes are achieved solely by changing the relative *phases* of the photoexcitation pulses that populate the electronic excited state by creating an initial coherent superposition. Similar control persists at larger values of S, where

the percentage product yield can be reduced from more than 30 % to less than 80 % by changing Θ from 0^o to $\sim 120^o$.

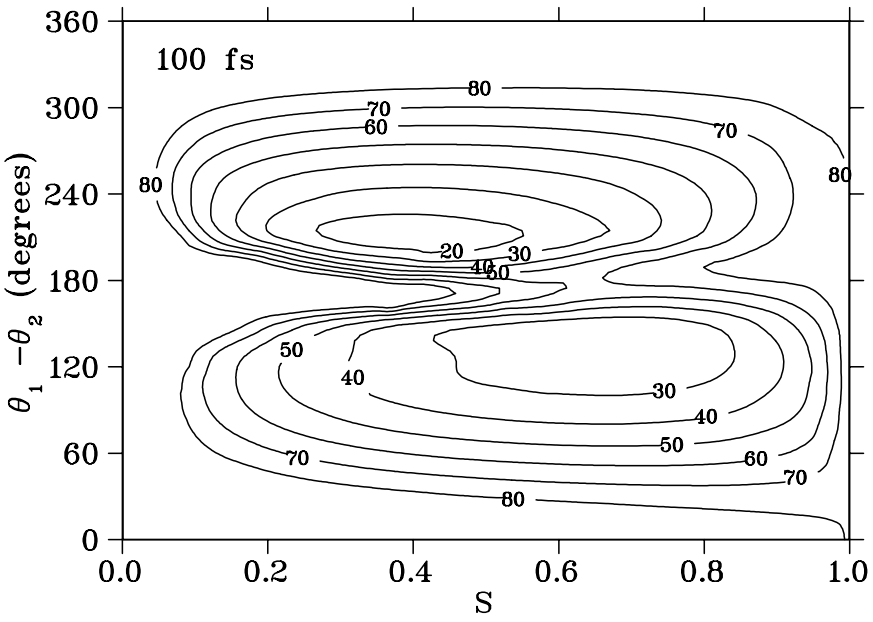

FIGURE 6. Contour plot of the percentage reactant for bichromatic coherent-control at 100 fs after photoexcitation of the system. Taken from Fig. 2, Ref. [**31**].

Figure 7 shows contour plots of the percentage product yields at 200 fs after excitation of the system. Here, the degree of yield control is maximum in the $0.2 < S < 0.8$ range, where the reactant probability can be reduced from more 80% to less than 40% by changing Θ from 120^o—180^o to 0^o.

The extent to which these results are significant is associated with the advent of intrinsic decoherence experienced by the proton during the course of the dynamics. To this end we examine the time dependence of $\mathrm{Tr}[\rho^2(t)]$, where $\rho(t)$ is the one-particle *reduced* density matrix associated with the proton, which serves as a decoherence measure[**41, 42, 43, 44**]. Further, we choose the initial state as the Gaussian ground vibrational state of the stretching mode associated with the *OH* bond (see Fig. 5) promoted to the first electronically excited state. Since the decoherence rate is expected[**44**] to increase with the configuration space size of the $\rho(0)$, this choice of initial condition should provide an approximate lower bound to the rate. Initially, $\mathrm{Tr}(\rho(0)^2) = 1$, indicative of a pure state. As the reaction proceeds, the proton becomes coupled to the remaining degrees of freedom in the system (i.e., a bath of 34 coupled modes) and $\mathrm{Tr}(\rho^2)$ is expected to decay.

Figure 8 shows $\mathrm{Tr}(\rho^2)$ as computed during the first 15 fs of dynamics. During this short time more than 98% of the population remains on the reactant side [**33**]. However, $\mathrm{Tr}(\rho^2)$ decays to ~ 0.6 by 4 fs (a time scale comparable to one half the period of the OH stretch in the enol tautomer). At this time the slope of the curve changes sign, indicating a change of the underlying physical process. Additional

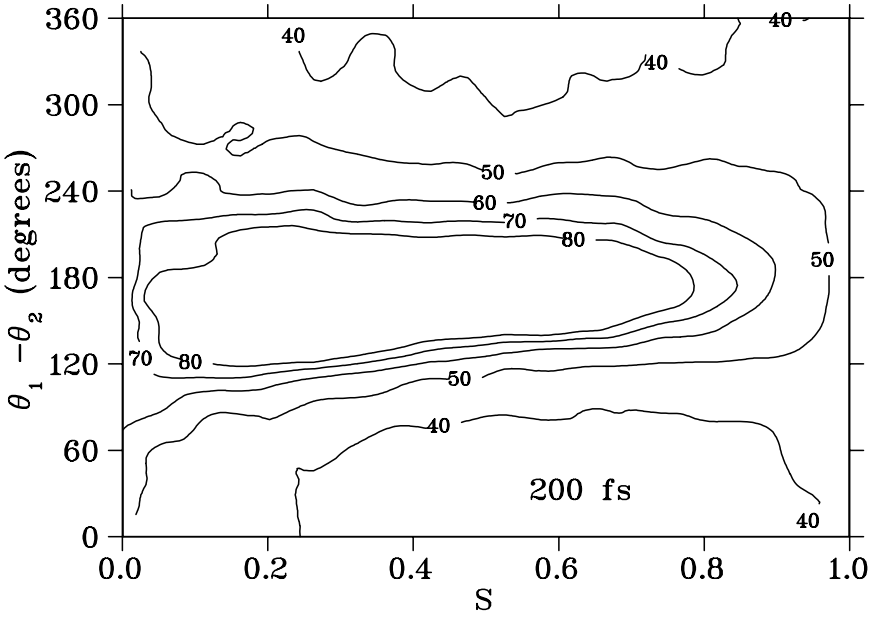

FIGURE 7. Contour plot of the percentage reactant for bichromatic coherent-control at 200 fs after photoexcitation of the system. Taken from Fig. 3, Ref. [**31**].

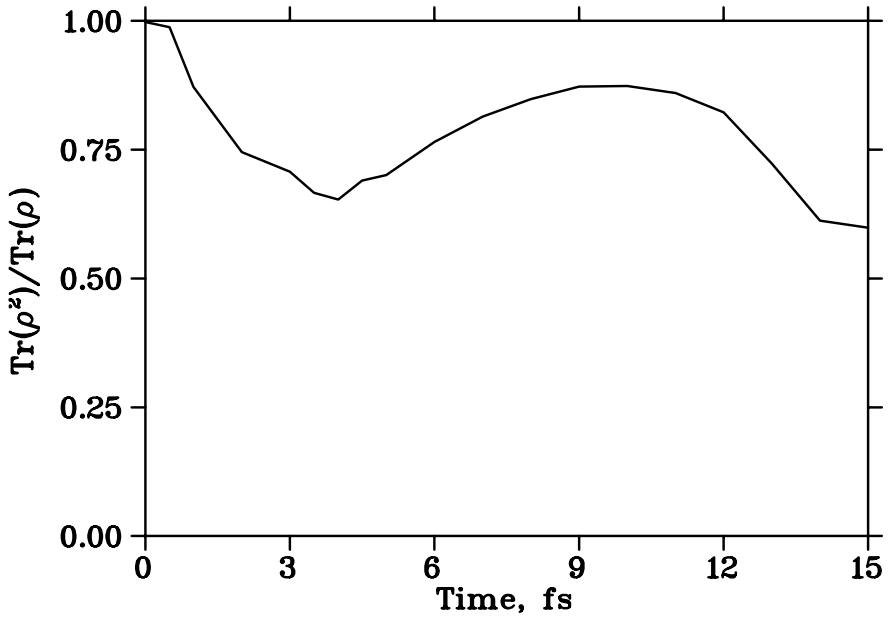

FIGURE 8. Trace of ρ^2 as a function of time during the first 15 fs of dynamics after photoexcitation of the system. Taken from Fig. 4, Ref. [**31**].

computations at longer times, specifically at 100 fs and 200 fs, show a further decrease of $\mathrm{Tr}(\rho^2)$ to 0.54 and 0.38, respectively. This is consistent with the fact that by 200 fs over 13% of the H-atom population has been transferred and that comparisons with fewer degree of freedom models[**33**] show that the dynamics beyond 100 fs involves coupling to a significant number of background modes. Figures 6 and 7 make clear that extensive coherent control is taking place in a system despite the ongoing decoherence.

It is important to note that these are benchmark state-of-the-art computations. Each time reported in Fig. 8 requires a separate calculation of a 140-dimensional integral using $\approx 10^7$ semiclassical trajectories. This considerable computational effort aims to produce the first explicit calculations of coherent-control in a system with many coupled degrees of freedom. To the best of our knowledge, our computations also constitute the first explicit calculations of a decoherence measure in a system with many degrees of freedom.

The essential nature of coherent control studies is such that we can now explore issues related to the detailed physics of the control mechanism. This includes an examination of the role of the initial mode prepared, the excitation duration and frequency content, etc. Such studies are underway.

8. Comments

Coherent control studies have provided deep insights into the nature of the quantum control of molecular processes. They highlight specific mechanisms that are responsible for the ability to control processes, providing the physical insight essential to scientific progress in the area. Numerous applications on small systems in a wide variety of areas have previously proven successful. The recent semiclassical study on HPO, summarized in this paper, makes clear that the future is bright for quantum control in large molecular systems, even though they experience decoherence effects.

References

[1] S. A. Rice and M. Zhao, *Optical Control of Molecular Dynamics*, Wiley, New York, 2000.
[2] M. Shapiro and P. Brumer, *Principles of the Quantum Control of Molecular Processes*, John Wiley and Sons, N.Y., in press.
[3] M. Shapiro and P. Brumer, J. Phys. Chem. 105, 2897 (2001)
[4] See, e.g., R. B. Bernstein, ed., *Atom-Molecule Collision Theory, A Guide for the Experimentalist*, Plenum Press, New York, 1979.
[5] M. Shapiro and P. Brumer, J. Phys. Chem. **105**, 2897 (2001).
[6] M. Shapiro, Adv. Chem. Phys. **114**, 123 (2000).
[7] R. S. Judson and H. Rabitz, Phys. Rev. Lett. **68**, 1500, (1992).
[8] C. J. Bardeen, V. V. Yakovlev, K. R. Wilson, S. D. Carpenter, P. M. Weber and W. S. Warren, Chem. Phys. Lett. **280**, 151 (1997).
[9] D. Yelin, D. Meshulach, Y. Silberberg, Opt. Lett. **22**, 1793 (1997).
[10] T. Assion, T. Baumert, M. Bergt, T. Brixner, B. Kiefer, V. Seyfried, M. Strehle and G. Gerber, Science **282**, 919 (1998).
[11] R.J. Levis, G.M. Menkir, H. Rabitz, Science **292**, 709 (2001)
[12] J. L. Herek, W. Wohlleben, R. J. Cogdell, D. Zeidler and M. Motzkus, Nature **417**, 533 (2002).
[13] P. Brumer and M. Shapiro, Chem. Phys. Lett. **126**, 541 (1986).
[14] M. Shapiro and P. Brumer, in *Advances in Atomic, Molecular and Optical Physics*, Vol. **42**, B. Bederson and H. Walther, ed., Academic Press, San Diego, 1999, pp. 287-343.
[15] M. Shapiro, J. Phys. Chem. **90**, 3644 (1986).

[16] P. Brumer and M. Shapiro, in *Coherent Control in Atoms, Molecules and Semiconductors*, W. Pötz and W.A. Schröder, ed., Kluwer, Dordrecht, 1999.
[17] D.J. Cook and R. M. Hochstrasser, Opt. Lett. **25**, 1210 (2000)
[18] M. Shapiro, E. Frishman and P. Brumer, Phys. Rev. Letters **84**, 1669 (2000)
[19] D. Gerbasi, M. Shapiro, and P. Brumer, J. Chem. Phys. **115**, 5349 (2001)
[20] P. Brumer, E. Frishman and M. Shapiro, Phys. Rev. A **65**, 015401 (2001)
[21] M. Shapiro, J. W. Hepburn and P. Brumer, Chem. Phys. Lett **149**, 451 (1988).
[22] C. Chen, Y-Y. Yin, and D.S. Elliott, Phys. Rev. Lett. **64**, 507 (1990); *ibid.*, **65**, 1737 (1990).
[23] S.M. Park, S-P. Lu, and R.J. Gordon, J. Chem. Phys. **94**, 8622 (1991).
[24] S-P. Lu, S.M. Park, Y. Xie, and R.J. Gordon, J. Chem. Phys. **96**, 6613 (1992).
[25] V.D. Kleiman, L. Zhu, X. Li and R.J. Gordon, J. Chem. Phys. **102**, 5863 (1995).
[26] L. Zhu, V.D. Kleiman, X. Li, S. Lu, K. Trentelman, and R.J. Gordon, Science **270**, 77 (1995).
[27] L. Zhu, K. Suto, J.A. Fiss, R. Wada, T. Seideman, and R.J. Gordon, Phys. Rev. Lett. **79**, 4108 (1997).
[28] R. J. Gordon, L. C. Zhu and T. Seideman, Acc. Chem. Res. **32**, 1007 (1999).
[29] J. Kupsch, in *Decoherence and the Appearance of the Classical World*, D. Giulini, E. Joos, C. Kiefer, J. Kupsch, I-O. Stamatescu and H. D. Zeh, ed., Springer-Verlag, New York, 1996.
[30] R. Omnes, *The Interpretation of Quantum Mechanics*, Princeton University Press, N.J., 1994.
[31] V.S. Batista and P. Brumer, Phys. Rev. Lett. **89**, 143201, (2002).
[32] M.F. Herman and E. Kluk, Chem. Phys. **91**, 27, (1984).
[33] V. Guallar, V.S. Batista and W. H. Miller, J. Chem. Phys. **113**, 9510 (2000).
[34] W.H. Miller, J. Phys. Chem. A **105**, 2942, (2001).
[35] V.S. Batista and P. Brumer, J. Chem. Phys. **114**, 10321 (2001).
[36] V.S. Batista and P. Brumer, J. Phys. Chem. **105**, 2591 (2001).
[37] T.C. Hesterberg, Technometrics **37**, 185, (1995).
[38] H.-D. Meyer, J. Chem. Phys. **84**, 3147 (1986).
[39] K.G. Kay, J. Chem. Phys. **101**, 2250 (1994).
[40] V. Guallar, V.S. Batista and W. H. Miller, J. Chem. Phys. **110**, 9922 (1999).
[41] P.C. Lichtner and J.J. Griffin, Phys. Rev. Lett. **37**, 1521, (1976).
[42] X-P. Jiang and P. Brumer, Chem. Phys. Lett. **208**, 179, (1993).
[43] W.H. Zurek, S. Habib and J.P. Paz, Phys. Rev. Lett. **70**, 1187, (1993).
[44] A. Pattanayak and P. Brumer, Phys. Rev. Lett. **79**, 4131, (1997).

Department of Chemistry, Yale University, New Haven, CT 06520-8107
E-mail address: victor.batista@yale.edu

Chemical Physics Theory Group, Department of Chemistry, University of Toronto, Toronto, Ontario, Canada M5S 3H6
E-mail address: pbrumer@tikva.chem.utoronto.ca